sensors

MDPI

Article

1 V Tunable High-Quality Universal Filter Using Multiple-Input Operational Transconductance Amplifiers

Montree Kumngern [1], Fabian Khateb [2,3,4,*], Tomasz Kulej [5] and Boonying Knobnob [6]

[1] Department of Telecommunications Engineering, School of Engineering, King Mongkut's Institute of Technology Ladkrabang, Bangkok 10520, Thailand; montree.ku@kmitl.ac.th
[2] Department of Microelectronics, Brno University of Technology, Technická 10, 601 90 Brno, Czech Republic
[3] Faculty of Biomedical Engineering, Czech Technical University in Prague, nám. Sítná 3105, 272 01 Kladno, Czech Republic
[4] Department of Electrical Engineering, Brno University of Defence, Kounicova 65, 662 10 Brno, Czech Republic
[5] Department of Electrical Engineering, Czestochowa University of Technology, 42-201 Czestochowa, Poland; kulej@el.pcz.czest.pl
[6] Faculty of Engineering, Rajamangala University of Technology Thanyaburi, Pathum Thani 12110, Thailand; kboonying@rmutt.ac.th
* Correspondence: khateb@vutbr.cz

Abstract: This paper presents a new multiple-input single-output voltage-mode universal filter employing four multiple-input operational transconductance amplifiers (MI-OTAs) and three grounded capacitors suitable for low-voltage low-frequency applications. The quality factor (Q) of the filter functions can be tuned by both the capacitance ratio and the transconductance ratio. The multiple inputs of the OTA are realized using the bulk-driven multiple-input MOS transistor technique. The MI-OTA-based filter can also offer many filtering functions without additional circuitry requirements, such as an inverting amplifier to generate an inverted input signal. The proposed filter can simultaneously realize low-pass, high-pass, band-pass, band-stop, and all-pass responses, covering both non-inverting and inverting transfer functions in a single topology. The natural frequency and the quality factors of all the filtering functions can be controlled independently. The natural frequency can also be electronically controlled by tuning the transconductances of the OTAs. The proposed filter uses a 1 V supply voltage, consumes 120 µW of power for a 5 µA setting current, offers 40 dB of dynamic range and has a third intermodulation distortion of −43.6 dB. The performances of the proposed circuit were simulated using a 0.18 µm TSMC CMOS process in the Cadence Virtuoso System Design Platform to confirm the performance of the topology.

Keywords: universal filter; voltage-mode circuit; operational transconductance amplifier

Citation: Kumngern, M.; Khateb, F.; Kulej, T.; Knobnob, B. 1 V Tunable High-Quality Universal Filter Using Multiple-Input Operational Transconductance Amplifiers. *Sensors* **2024**, *24*, 3013. https://doi.org/10.3390/s24103013

Academic Editor: Pak Kwong Chan

Received: 22 April 2024
Revised: 4 May 2024
Accepted: 6 May 2024
Published: 9 May 2024

1. Introduction

An operational transconductance amplifier (OTA) is a voltage-controlled current source that offers numerous advantages in circuit design, such as providing electronic tuning capability, easy implementation of the OTA structure, and the powerful ability to realize various applications. In addition, OTA-based circuits are usually absent from resistor requirements, making them suitable for integrated circuit (IC) implementation [1,2].

Biquad filters are very useful blocks for applications in measurement, communication, and control systems. From the general form of second-order filter functions [3], there are five frequency responses that are possible to obtain, namely low-pass filter (LPF), high-pass filter (HPF), band-pass filter (BPF), band-stop filter (BSF), and all-pass filter (APF). These are the so-called five standard filtering functions. A biquad filter can be used to realize high-order filters by cascading multiple first-order and second-order sections, as used in phase-lock loops (PLL) for loop filtering (usually an LP filter), FM stereo demodulators (usually LP and BP filters), and crossover networks in three-way high fidelity (usually LP,

BP, and HP filters) [3]. A filter that can provide several second-order filters in a single topology is classified as a universal filter. There are many universal filters available in the literature using varying active devices, such as second-generation current conveyors (CCIIs) [4–6] and current feedback operational amplifiers (CFOAs) [7–9]. Unfortunately, these filters lack electronic tuning capabilities, which is important when parameters such as the natural frequency and quality factor deviate by process–voltage–temperature (PVT) variations. Some universal filters that offer the possibility of electronic tuning and minimal active elements have been introduced by using the voltage differencing inverting buffered amplifier (VDIBA) [10,11] and inverters [12]. However, these filters supply the input signals through capacitors, and therefore, an additional buffer circuit is required, and these capacitors become floating.

This work is focused on a universal filter with electronic tuning capability that utilizes an operational transconductance amplifier (OTA) as the active element. There are many universal filters using OTAs as active elements available in the literature; for example, see [13–49]. The circuits in [13–16] are current-mode filters, the circuits in [17–35] are voltage-mode filters, and the circuits in [35–42] are mixed-mode filters. Considering the input and output terminals, the circuits in [17–22,39] are single-input multiple-output (SIMO) filters, the circuits in [15,16,23–29,40,41] are multiple-input single-output (MISO) filters, and the circuits in [13,14,30–38,42] are multiple-input multiple-output (MIMO) filters. Compared with SIMO filters, MISO and MIMO filters usually employ fewer active devices because the variant filtering functions of these filters can be obtained by appropriately selecting the input and/or output terminals. This work is focused on utilizing the MISO filter so that parameters such as the natural frequency and the quality factor can be electronically and independently controlled. Considering the MIMO and MISO filters in [13–16,23–38,40–42], these filters suffer from some drawbacks:

(i) They require additional circuits at the input, such as a SIMO current follower circuit [13–16].
(ii) They use a floating capacitor or floating resistor [23,28,31,32].
(iii) They do not provide the non-inverting and inverting transfer functions of LP, HP, BP, BS, and AP filters [23–38,40,41].
(iv) They do not provide independent tunable control of the natural frequency and the quality factor [23–25,27,29–33,38,40,41].
(v) They require inverted input signals to obtain some transfer functions [24,31,37,38].

It should be noted that these universal filters are not designed for low-voltage low-power signal-processing applications. Nowadays, low-voltage low-power filters are required for biomedical applications, such as biosensors [3]. Universal filters using OTAs operating with a low supply voltage and with low power consumption are available in the literature [42–47]. However, these configurations cannot benefit from independent and electronic control of the quality factor and the natural frequency and cannot provide a high-quality (high-Q) filter. In modern applications, high-Q filters are strictly desirable for processing weak signals, such as the detection, measurement, and quantification of biomedical signals [48,49]. The bio-signal has the attributes of a low amplitude and a low frequency ($\leq$10 kHz).

This paper presents a low-voltage low-power universal biquadratic filter that allows the natural frequency and quality factor to be independently and electronically controlled. A high-Q filter can also be obtained. The filter is realized using multiple-input operational transconductance amplifiers (MI-OTAs). In the filter's input differential stage, the MI-OTAs are realized using the multiple-input MOS transistor technique (MI-MOST), which obtains a minimal differential pair and minimal power consumption. Using an MI-OTA-based filter shows that both the non-inverting and the inverting transfer functions of LP, HP, BP, BS, and AP filters can be obtained without inverted input signals. The proposed filter uses a 1 V supply voltage and 120 μW of power consumption for a 5 μA setting current. The filter was designed and simulated in the Cadence Virtuoso environment using 0.18 μm TSMC CMOS technology.

2. Circuit Description

2.1. Multiple-Input OTA

The multiple-input OTA is used to realize the filter application. Its circuit symbol is shown in Figure 1. Ideally, the transfer characteristic of this OTA is given by the following equation:

$$I_o = g_m(V_{+1} + V_{+2} + \ldots + V_{+n} - V_{-1} - V_{-2} - \ldots - V_{-n}) \quad (1)$$

where I_o is the output current, and g_m is the small-signal transconductance. Note that the circuit in the general case has n non-inverting and n inverting inputs; thus, its input voltage can be considered as the difference of two sums of voltages applied to the non-inverting $V_{+1,\ldots,+n}$ and inverting $V_{-1,\ldots,-n}$ inputs, respectively.

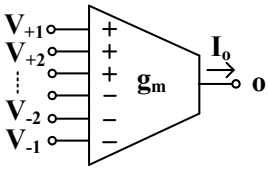

Figure 1. Electrical symbol of the MI-OTA.

The transistor-level schematic of the OTA proposed in this work with n = 3 is shown in Figure 2. The circuit consists of an OTA with folded-cascode topology with a linearized input stage consisting of the transistors M_1–M_2 and M_{1SD}, M_{2SD}, and biased by the current sinks M_3 and M_4. The transistors M_{13}–M_{18} were used for biasing. The multiple inputs were realized in a simple way by adding a capacitive voltage divider to the transistors M_1 and M_2, thus creating a multiple-input device, as shown in Figure 3. The input capacitors C_{Bi} were bypassed by large R_{MOSi} resistances, which were realized as an anti-parallel connection of MOS transistors operating in a cutoff region. The large resistances provided the DC biasing of the M_1 and M_2 gates.

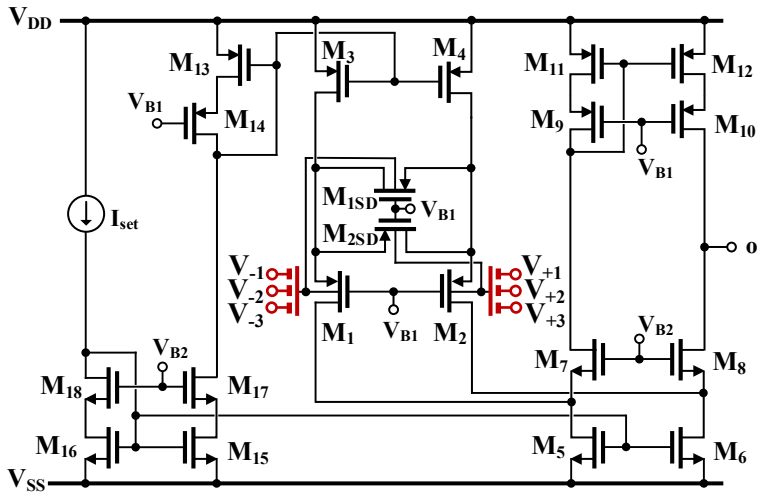

Figure 2. CMOS realization of the MI-OTA using the MIBD-MOST technique.

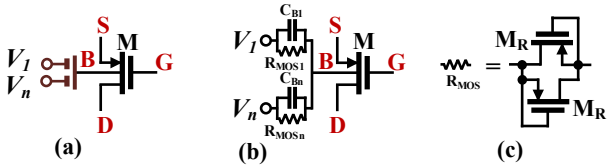

Figure 3. The MIBD-MOST technique: (**a**) symbol, (**b**) realization, and (**c**) R_{MOS} realization.

The linearization technique used in this work is similar to the technique with gate-driven input stages operating in strong inversion introduced in [50]. However, in this work,

the bulk-driven devices operating in weak inversion were applied to the proposed structure. Operation in weak inversion generally leads to a narrower linear range compared to the strong inversion version of the circuit. On the contrary, the use of bulk-driven terminals extends the linear range compared to the gate-driven realization. Moreover, the input capacitive divider further extends the linear range. The result is the relatively large linear range of the OTA, even for weakly inverted devices biased with very low currents. A similar input stage was first described and verified experimentally in [51,52]. The M_{1SD} and M_{2SD} transistors operate in a triode region, introducing negative feedback to the input pair M_1 and M_2. Controlling their characteristics by the signals seen at the gates of the main transistors of the pair M_1 and M_2 further improves the linearity of the input stage [51].

Assuming that all the capacitances C_{Bi} are identical, the small-signal transconductance of the OTA is given by:

$$g_m = \frac{\eta}{n} \cdot \frac{4k}{4k+1} \cdot \frac{I_{set}}{n_p U_T} \tag{2}$$

where $\eta = g_{mb1,2}/g_{m1,2}$ is the bulk to gate transconductance ratio at the operating point, n is the number of input terminals, n_p is the subthreshold slope factor for the p-channel transistors, U_T is the thermal potential, I_{set} is the biasing current and k is the ratio of aspect ratios of the triode-region transistors M_{1SD}, M_{2SD} and the main transistors of the input pair M_1 and M_2:

$$k = \frac{(W/L)_{1SD,2SD}}{(W/L)_{1,2}} \tag{3}$$

Note that the best linearity performance is obtained for k = 0.5 [51]. In such a case, the circuit transconductance can be expressed as:

$$g_m = \frac{2}{3} \cdot \frac{\eta}{n} \cdot \frac{I_{set}}{n_p U_T} \tag{4}$$

The use of an input capacitive divider and bulk-driven devices extends the linear range of the OTA, but on the other hand, it increases the input noise and decreases the voltage gain. For instance, with $\eta = 1/3$ and 3 inputs, the circuit transconductance is lowered 9 times as compared to a gate-driven input pair. Consequently, the low-frequency voltage gain of the circuit is decreased by around 19 dB. To counteract this effect, we applied a cascode high-impedance output stage, composed of the transistors M_5–M_{12}. With the applied output stage, the low-frequency gain of the OTA can be approximated as:

$$A_V \cong g_m[(g_{m8} r_{ds8} r_{ds6}) || (g_{m10} r_{ds10} r_{ds12})] \tag{5}$$

Consequently, this gain is improved by the factor of $g_m r_{ds}$ (intrinsic voltage gain of an MOS transistor), which for the applied technology and operating point exceeds 30 dB.

As was already mentioned, the applied technique increases the linear range of the OTA. On the other hand, however, it increases its input noise due to signal attenuation. Since the input noise is increased in the same proportion, the dynamic range (DR) of the OTA remains unchanged and is equal to the DR of the GD OTA with a single differential input and the applied linearization technique. Nevertheless, the larger linear range allows for avoiding hard nonlinearities for the large voltage swings and V_{DD}, as applied in the considered design.

2.2. Proposed Tunable High-Q Voltage-Mode Universal Filter

Figure 4 shows the proposed tunable high-*Q* voltage-mode universal filter using OTAs. Figure 4a shows the proposed voltage-mode universal filter using conventional OTAs and Figure 4b shows the proposed voltage-mode universal filter using MI-OTAs. It should be noted from Figure 4a,b that the universal filter using MI-OTAs has a significantly reduced number of OTAs (10 OTAs vs. 4 MI-OTAs). The input terminals of the universal filter in Figure 4b are connected to the high-input impedance of the OTA; thus, the proposed

universal filter offers high input impedance, which is ideal for voltage-mode circuits. The output impedance can be given by $1/g_{m4}$.

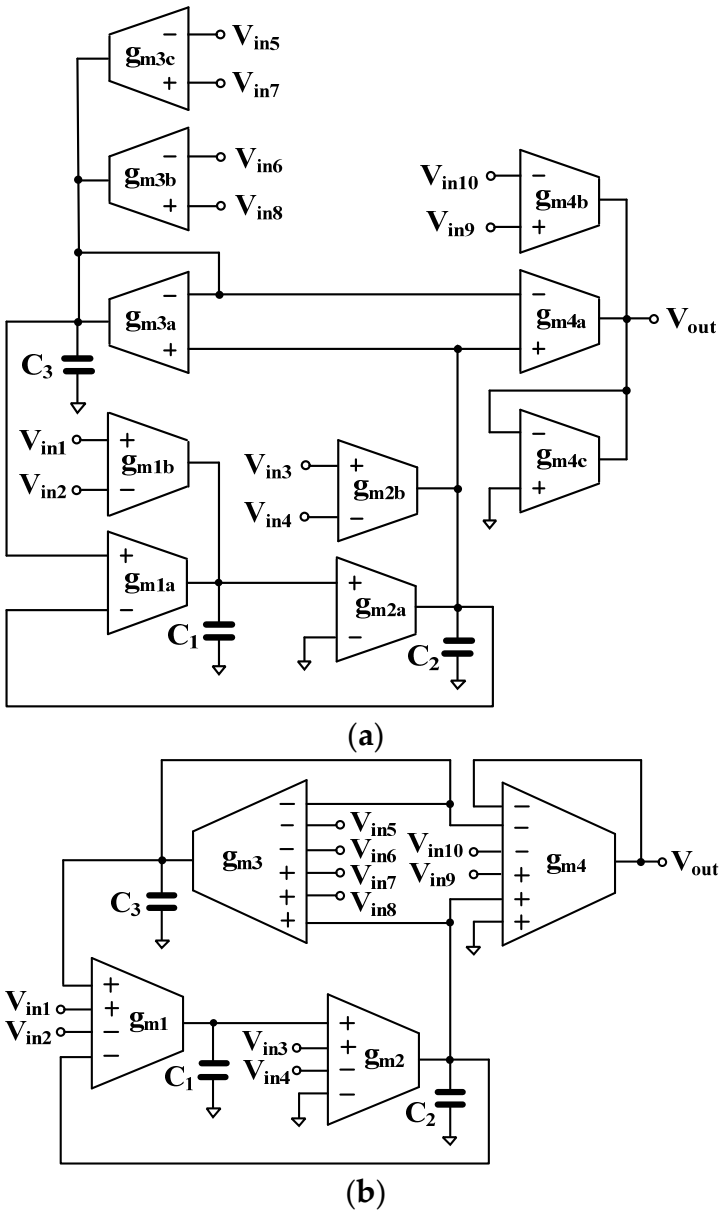

Figure 4. Proposed tunable high-Q voltage-mode universal filter using (**a**) conventional OTAs and (**b**) MI-OTAs.

Letting $g_{m1a} = g_{m1b} = g_{m1}$, $g_{m2a} = g_{m2b} = g_{m2}$, $g_{m3a} = g_{m3b} = g_{m3c} = g_{m3}$, $g_{m4a} = g_{m4b} = g_{m4c} = g_{m4}$, and using nodal analysis, the output voltage of Figure 4a,b can be given by:

$$V_{out} = \frac{\left\{\begin{array}{c} g_{m1}g_{m2}(V_{in1} - V_{in2}) + sC_1g_{m2}(V_{in3} - V_{in4}) \\ +s\frac{C_1C_2g_{m3}}{C_3}(V_{in5} + V_{in6} - V_{in7} - V_{in8}) \\ +D(s)(V_{in9} - V_{in10}) \end{array}\right\}}{D(s)} \quad (6)$$

where $D(s) = s^2C_1C_2 + s\frac{C_1C_2g_{m3}}{C_3} + g_{m1}g_{m2}$.

The variant filtering functions are shown in Table 1. It should be noted that the variant non-inverting and inverting transfer functions of the LPF, BPF, HPF, BSF, and APF can be obtained without inverted input signal requirements. For the BPF, if the input signals are

V_{in3} and V_{in4}, varying the quality factor will increase the gain of the transfer functions. Conversely, if the input signals are V_{in5} or V_{in6} and V_{in7} or V_{in8}, varying the quality factor will not affect the gain of the transfer functions.

Table 1. Obtaining the variant filtering functions of the proposed universal filter.

Filtering Function		Input
LPF	Non-inverting	V_{in1}
	Inverting	V_{in2}
BPF	Non-inverting	V_{in3}
	Inverting	V_{in4}
	Non-inverting	V_{in5} or V_{in6}
	Inverting	V_{in7} or V_{in8}
HPF	Non-inverting	$V_{in2} = V_{in7} = V_{in9}$
	Inverting	$V_{in1} = V_{in5} = V_{in10}$
BSF	Non-inverting	$V_{in7} = V_{in9}$
	Inverting	$V_{in5} = V_{in10}$
APF	Non-inverting	$V_{in7} = V_{in8} = V_{in9}$
	Inverting	$V_{in5} = V_{in6} = V_{in10}$

Letting $V_{in7} = V_{in8} = V_{in9} = V_{in}$, $V_{out} = V_{AP+}$, the transfer function of the non-inverting APF can be expressed as in (7), and letting $V_{in5} = V_{in6} = V_{in10} = V_{in}$, $V_{out} = V_{AP-}$, the transfer function of the inverting APF can be expressed as in (8).

$$\frac{V_{AP+}}{V_{in}} = \frac{s^2C_1C_2 - s\frac{C_1C_2g_{m3}}{C_3} + g_{m1}g_{m2}}{s^2C_1C_2 + s\frac{C_1C_2g_{m3}}{C_3} + g_{m1}g_{m2}} \tag{7}$$

$$\frac{V_{AP-}}{V_{in}} = \frac{-s^2C_1C_2 + s\frac{C_1C_2g_{m3}}{C_3} - g_{m1}g_{m2}}{s^2C_1C_2 + s\frac{C_1C_2g_{m3}}{C_3} + g_{m1}g_{m2}} \tag{8}$$

These transfer functions can be used to express the magnitudes and phase responses of APFs.

The natural frequency (ω_o) and the quality factor (Q) can be given by:

$$\omega_o = \sqrt{\frac{g_{m1}g_{m2}}{C_1C_2}} \tag{9}$$

$$Q = \frac{C_3}{g_{m3}}\sqrt{\frac{g_{m1}g_{m2}}{C_1C_2}} \tag{10}$$

The parameter ω_o can be controlled electronically by g_{m1} and g_{m2} and the parameter Q can be controlled by C_3 and/or g_{m3}. If C_3 is used as a parameter, C_1 and C_2 could be constant ($C_1 = C_2$), and if g_{m3} is used as a parameter, g_{m1} and g_{m2} could be constant ($g_{m1} = g_{m2}$). Thus, the parameter Q can be tuned by varying the values of the capacitance and resistance.

2.3. Effects of the Nonidealities of the MI-OTA

Figure 5 shows the nonideal model of the OTA [53]. There are three components that have been considered: (i) the input capacitances C_+, C_-, and input resistances R_+, R_-; (ii) the output capacitance C_o and output resistance R_o (or conductance g_o); and (iii) the frequency-dependent transconductance g_m.

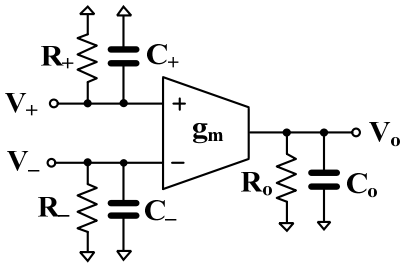

Figure 5. Nonideal structure of the OTA.

The frequency-dependence of g_m (g_{mn}) can be approximated [54] as:

$$g_{mn} = g_m(1 - s\tau) \tag{11}$$

where $\tau = 1/\omega_p$ and ω_p denotes the second pole of the OTA.

The first consideration can be rewritten by using (9) and the denominator of (6) as:

$$\begin{array}{c} s^2C_1C_2\left(1 - \frac{g_{m3}\tau_3}{C_3} + \frac{g_{m1}g_{m2}\tau_1\tau_2}{C_1C_2}\right) \\ +s\frac{C_1C_2g_{m3}}{C_3}\left(1 - \frac{C_3g_{m1}g_{m2}}{C_1C_2g_{m3}}(\tau_1 - \tau_2)\right) + g_{m1}g_{m2} \end{array} \tag{12}$$

It can be seen that the parasitic poles (τ_i) of the i-th OTA affect the filter performance. The influence of the parasitic pole can be neglected if the following conditions are met:

$$\left.\begin{array}{l} \frac{g_{m3}\tau_3}{C_3} + \frac{g_{m1}g_{m2}\tau_1\tau_2}{C_1C_2} \ll 1 \\ \frac{C_3g_{m1}g_{m2}}{C_1C_2g_{m3}}(\tau_1 - \tau_2) \ll 1 \end{array}\right\} \tag{13}$$

Next, the parasitic capacitances and resistances (or conductance) have been considered by letting the transconductance g_m be ideal. Considering Figure 4b, the values of the capacitors C_1, C_2, and C_3 can be represented, respectively, by C_1', C_2', and C_3', where $C_1' = C_1 + C_{o1} + C_{+2}$, $C_2' = C_2 + C_{o2} + C_{-1} + C_{+3} + C_{+4}$, and $C_3' = C_3 + C_{o3} + C_{+1} + C_{-3} + C_{-4}$, where C_{oj} is the output capacitance of the j-th g_m, and C_{+j} and C_{-j} are the input capacitances of the j-th g_m (j = 1, 2, 3, 4).

When the parasitic resistances are considered, the capacitors C_1', C_2', and C_3' are expressed, respectively, by C_1'', C_2'', and C_3'', where $C_1'' = C_1'//R_{o1}//R_{+2}$, $C_2'' = C_2'//R_{o2}//R_{-1}//R_{+3}//R_{+4}$, $C_3'' = C_3'//R_{o3}//R_{+1}//R_{-3}//R_{-4}$, where R_{oj} is the output resistance of the j-th g_m, R_{+j} and R_{-j} are the input resistances of the j-th g_m (j = 1, 2, 3, 4).

The parasitic effects on the natural frequency and the quality factor of the proposed universal filter can be avoided by choosing:

$$\left.\begin{array}{l} C_1 \gg (C_{o1} + C_{+2}) \\ C_2 \gg (C_{o2} + C_{-1} + C_{+3} + C_{+4}) \\ C_3 \gg (C_{o3} + C_{+1} + C_{-3} + C_{-4}) \end{array}\right\} \tag{14}$$

3. Simulation Results

The proposed MI-OTA and the filter application were simulated in the Cadence Virtuoso System Design Platform using the 0.18 μm CMOS technology from TSMC (Taiwan Semiconductor Manufacturing Company, Taiwan). The aspect ratio of the MOS transistors of the MI-OTA in Figure 1 is listed in Table 2. The voltage supply was 1 V ($V_{DD} = -V_{SS} = 0.5$ V). The proposed MI-OTA consumed 30 μW for a 5 μA setting current.

Table 2. Parameters of the components of the MI-OTA.

Transistor	W/L (μm/μm)
M_1–M_4, M_{13}–M_{18}	10/0.5
M_{1SD}, M_{2SD}	5/0.5
M_5–M_{12}	20/0.5
M_R	4/5
C_B = 0.5 pF	
V_{B1} = −300 mV, V_{B2} = 200 mV	

The parasitic impedances of the MI-OTA are shown in Figure 6, where $R_{+,-}$ = 42 GΩ, $C_{+,-}$ = 0.25 pF for the input terminal, and R_o = 32.4 MΩ, C_o = 52.8 fF for the output terminal.

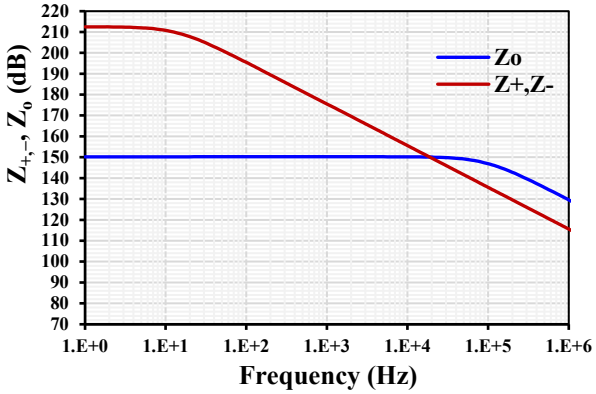

Figure 6. The parasitic impedances of the MI-OTA.

To obtain the dynamic characteristic of the MI-OTA, a sine wave of 1 kHz was applied to the input of the OTA. The extended linearity of the MI-OTA with various setting currents I_{set} = (2.5, 5, 10, 20) μA is shown in Figure 7a. The transconductance AC characteristic of the MI-OTA with various setting currents I_{set} = (2.5, 5, 10, 20) μA is shown in Figure 7b. The transconductance was (2.9, 4.9, 7.9, 12.6) μS, respectively. The transconductance AC characteristic with I_{set} = 5 μA was repeated for the Monte Carlo (MC) analysis with 200 runs and process, voltage, and temperature (PVT) corners, as shown in Figure 8.

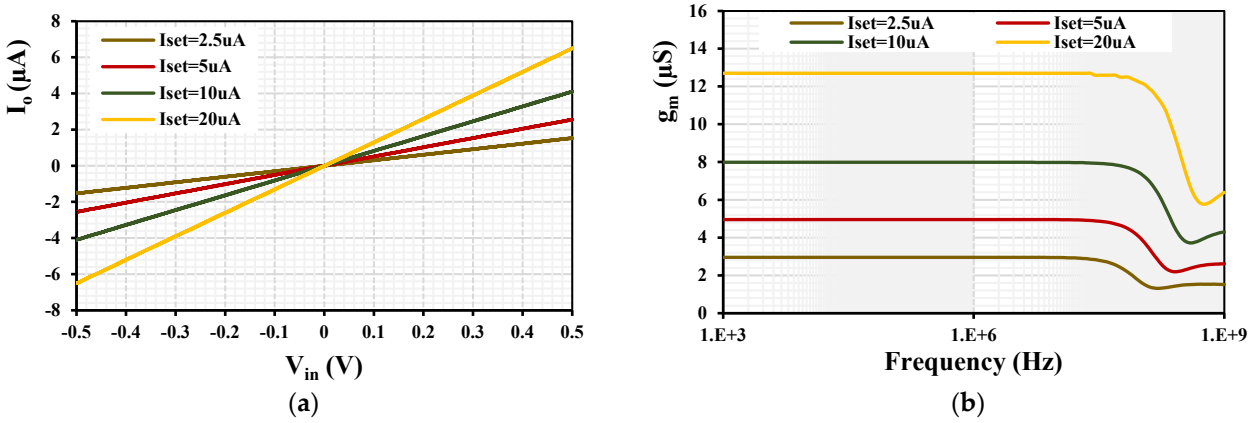

Figure 7. The I_o versus V_{in} (**a**) and the transconductance AC characteristic (**b**) with different setting currents.

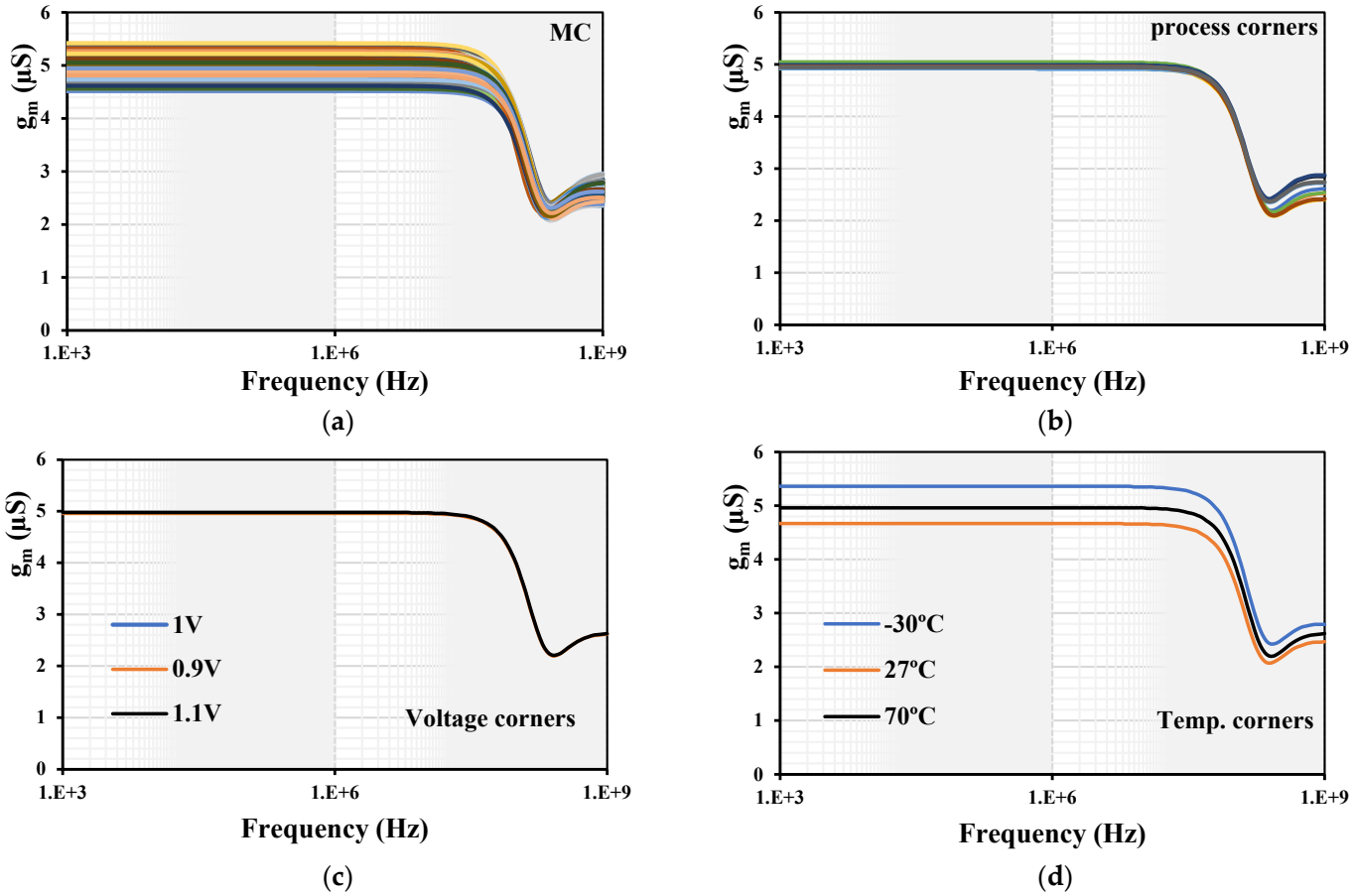

Figure 8. The transconductance AC characteristic of the MI-OTA: (**a**) MC, (**b**) process, (**c**) voltage and (**d**) temperature corners.

The process corners of the transistor were fast–fast, fast–slow, slow–fast, and slow–slow. For the input MIM capacitor C_B, they were fast–fast and slow–slow. The voltage corners were $V_{DD} \pm 10\%$, and the temperature corners were −30 °C and 70 °C. The MC showed min. 4.5 µS and max. 5.4 µS. The process corners showed min. 4.91 µS and max. 5 µS. The temperature corners showed min. 4.66 µS and max. 5.36 µS. The voltage corners showed min. 4.94 µS and max. 4.97 µS. All the transconductance variations were in the acceptable range. The frequency and phase characteristics of the filter with $I_{set1–4}$ = 5 µA and $C_{1–3}$ = 100 pF are shown in Figure 9. The cutoff frequency was 7.85 kHz. The simulation of the LPF was repeated with MC and PVT corners analyses, as shown in Figure 10. While the curves for the PVT overlapped, for the MC, the gain variation at low frequencies was in the range of −3.1 dB to 1.6 dB and the cutoff frequency variation was in the range of 0.72 kHz to 9.3 kHz, which can be realigned by adjusting the setting current.

To demonstrate the tuning capability of the *Q*, Figure 11 shows the frequency characteristics of the BPF with: (a) $I_{set1–4}$ = 5 µA, $C_{1,2}$ = 100 pF and tuning C_3 = (25, 50, 100, 200, 400, 800) pF and (b) with $I_{set1,2,4}$ = 5 µA, $C_{1–3}$ = 100 pF and tuning I_{set3} = (0.3125, 0.625, 1.25, 2.5, 5, 10) µA. To demonstrate the tuning capability of the ω, Figure 12 shows the frequency characteristics of the BPF with $C_{1–3}$ = 100 pF and tuning I_{set} = $I_{set1–4}$ = (0.3125, 0.625, 1.25, 2.5, 5, 10) µA. The natural frequency was (0.767, 1.44, 2.63, 4.62, 7.85, 12.7) kHz, respectively.

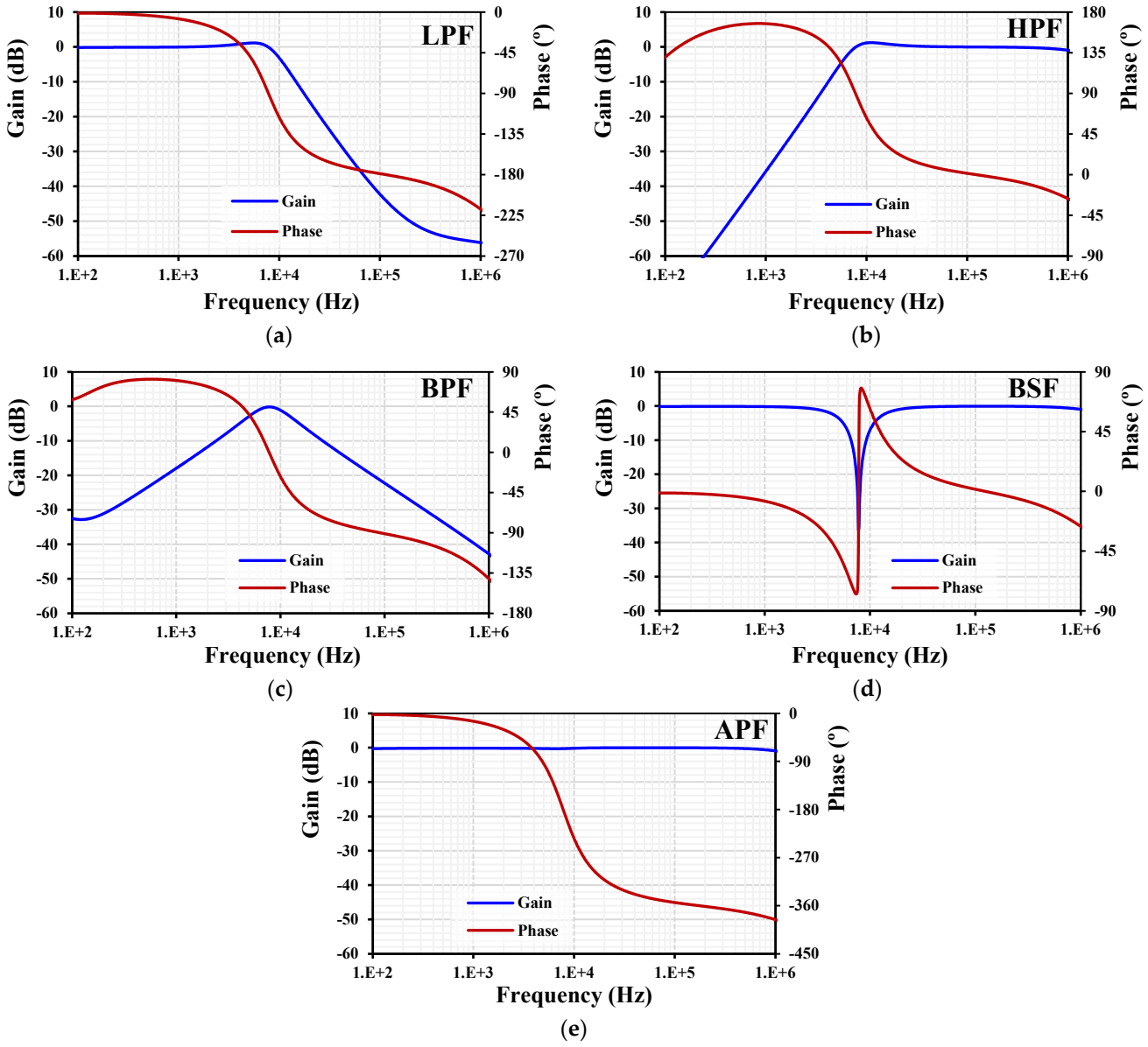

Figure 9. The frequency and phase characteristics of the filter.

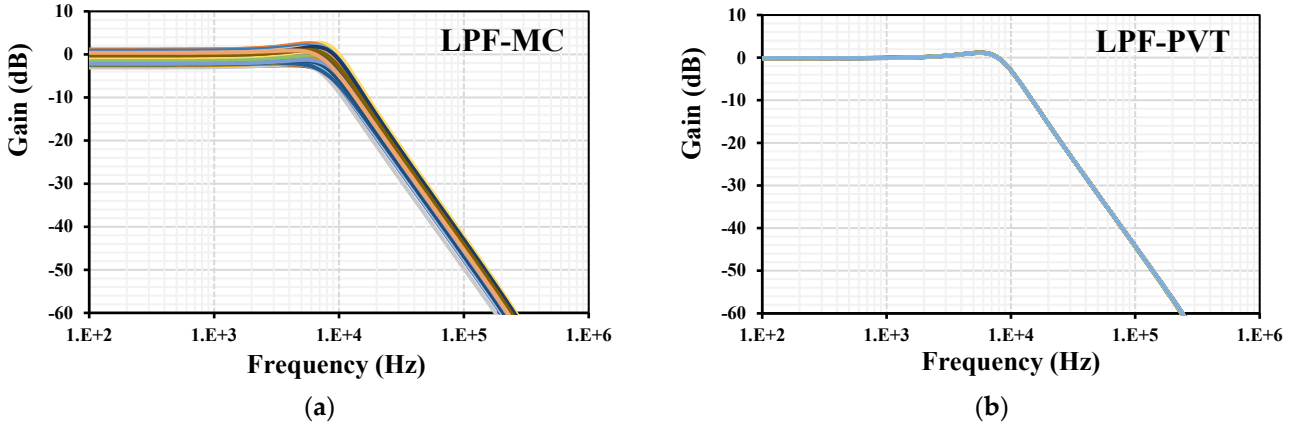

Figure 10. The frequency characteristics of the LP filter with (**a**) MC analysis and (**b**) PVT corners.

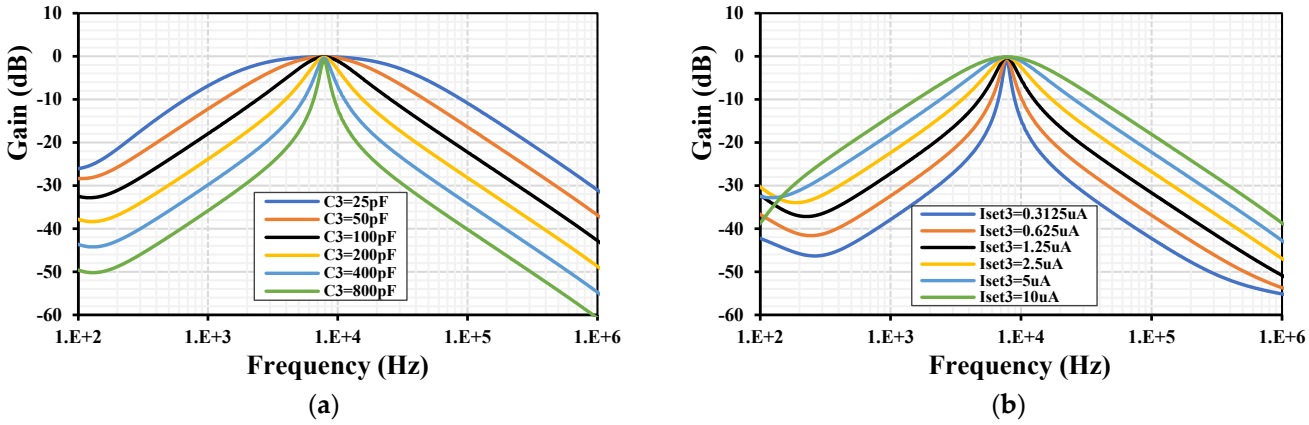

Figure 11. The frequency characteristic of the BPF with different values for (**a**) the capacitor C_3 and (**b**) the setting current I_{set3}.

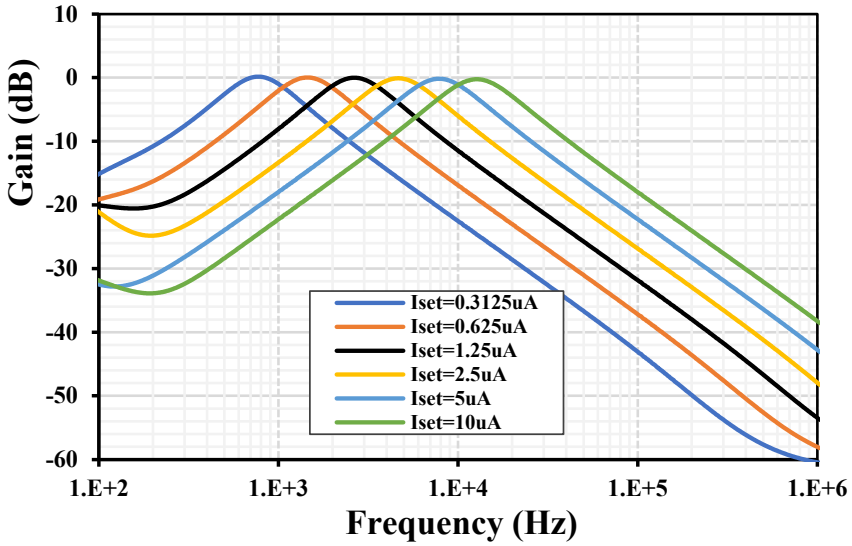

Figure 12. The frequency characteristic of the BPF with different $I_{set1–4}$.

To determine the third intermodulation distortion (IMD3) of the BPF, two closed tones were applied to the input of the BPF. Both tones were a sine wave with an amplitude of 25 mV but with different frequencies: 7.5 kHz and 8.2 kHz. The transient analyses of the input and output signal are shown in Figure 13a and the spectrum of the output signal is shown in Figure 13b. The IMD3 was −43.6 dB, which indicates a 0.66% THD.

The equivalent output noise is shown in Figure 14. The integrated noise in the filter bandwidth of 4.8 kHz to 12.5 kHz was 485.7 μV; hence, the dynamic range DR was calculated to be 40 dB for 1% IMD3.

The OTA-based universal filters in [16,34,41,45,46] were used as a comparison, as shown in Table 3. Compared with the filters in [16,34], which offer independent/electronic control of the ω_o and Q as well as a high-Q filter, the proposed filter offers larger transfer functions that cover both the non-inverting and the inverting transfer functions of the LPF, HPF, BPF, BSF, and APF. Compared with the filters in [41,45,46], which provide sub-volt supply voltage, the proposed filter offers independent/electronic control of the ω_o and Q and a high-Q filter. Compared with the filters in [16,34,41], the proposed filter offers low voltage and low power consumption.

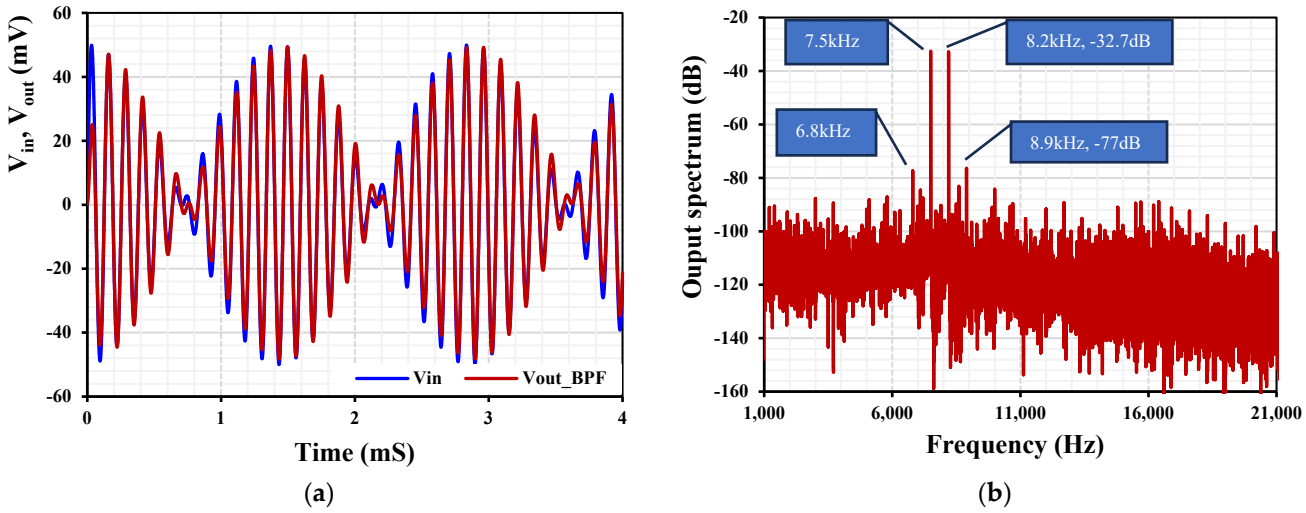

Figure 13. (**a**) The transient characteristic of the BPF and (**b**) the spectrum of the output signal.

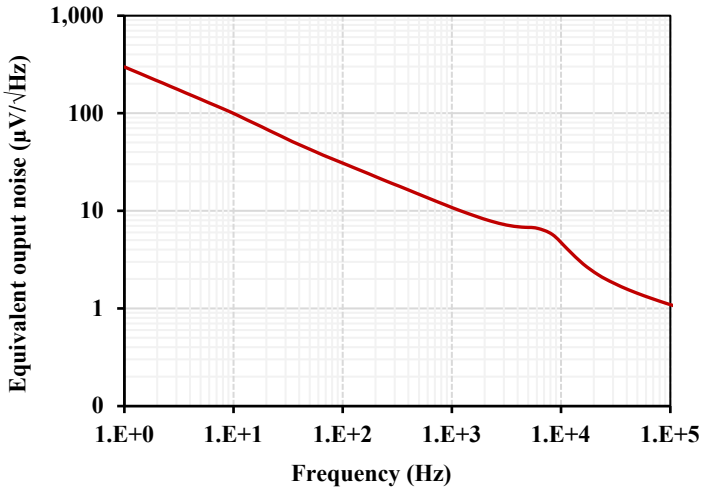

Figure 14. The output noise of the BPF.

Table 3. Comparison of the properties of this work with those of high-*Q* universal filters.

Factor	Proposed	[16] 2010	[34] 2019	[41] 2020	[45] 2022	[46] 2022
Number of active devices	4-OTA	3-OTA	5-OTA	5-OTA	8-OTA	3-OTA
Realization	0.18 μm CMOS	BJT (AT&T CBIC-R)	Commercial IC (LT1228)	0.18 μm CMOS	0.18 μm CMOS	0.18 μm CMOS
Number passive devices	3-C	3-C	2-C	2-C	2-C	2-C
Type of filter	MISO	MISO	MIMO	MISO	MIMO	MIMO
Total number of offered responses	12 (VM)	5 (CM)	7 (VM)	20 (MM)	20 (MM)	22 (VM)
Electronic control of ω_o	Yes	Yes	Yes	Yes	Yes	Yes
Independent control of Q	Yes	Yes	Yes	No	No	No
High-Q filter	Yes	Yes	Yes	No	No	No
All-grounded passive devices	Yes	Yes	Yes	Yes	Yes	Yes
High input impedances	Yes	-	Yes	Yes	Yes	Yes

Table 3. *Cont.*

Factor	Proposed	[16] 2010	[34] 2019	[41] 2020	[45] 2022	[46] 2022
Unnecessary input-matching conditions	Yes	No	Yes	Yes	Yes	Yes
Unnecessary inverted input signal	Yes	No	Yes	Yes	Yes	Yes
Achievable range of *Q*-factor	0.26 to 9.7 [a] 0.62 to 9.7 [b]	1 to 64 [c] 1 to 64 [d]	1.02 to 3.03 [e]	-	-	-
Power supply (V)	1	±2	±15	±0.9	±0.3	0.5
Power dissipation (nW)	120×10^3	-	861×10^6	177.3×10^3	5770	37
Natural frequency (kHz)	7.85	1000	159.16	3.39×10^3	5	0.153
Total harmonic distortion (%)	1@140mV$_{pp}$	-	-	-	<2@200mV$_{pp}$	0.33@100mV$_{pp}$
IMD3	−43.6 dB	-	−43.6 dBc	-	-	-
Output integrated noise (μVrms)	485.7	-	-	-	115	220
Dynamic range (dB)	40	-	-	-	53.2	50
Verification of result	Sim	Sim	Sim/Exp	Sim	Sim	Sim

Note: [a] = the capacitance varies from 25 to 800 pF, [b] = the biasing current varies from 0.312 to 10 μA, [c] = the capacitance varies from 2 to 128 nF, [d] = the biasing current varies from 1 to 70 μA, [e] = the g_m varies from 1 to 3 mS.

4. Conclusions

In this paper, a new multiple-input single-output voltage-mode universal filter using MI-OTAs is proposed. In this filter, the pole-*Q* can be tuned by varying the capacitance and setting current. The natural frequency can also be electronically controlled. The proposed filter uses four MI-OTAs that its differential pair realizes using the multiple-input MOS transistor technique, which does not increase the power consumption of the OTA. This work shows that an MI-OTA-based filter with 10 transfer functions, namely the non-inverting and inverting transfer functions of the LPF, HPF, BPF, BSF, and APF, can be obtained without changing the circuit topology. The proposed filter is suitable for low-voltage-supply, low-power-consumption and low-frequency applications like the biomedical one, since it is capable of operating with a 1 V supply voltage and consumes 120 μW of power for a 5 μA setting current.

Author Contributions: Conceptualization, M.K., F.K. and T.K.; methodology, M.K., F.K. and T.K.; software, M.K. and F.K.; validation, M.K., F.K. and B.K.; formal analysis, M.K. and T.K.; investigation, M.K., F.K. and T.K.; resources, M.K.; data curation, M.K. and F.K.; writing—original draft preparation, M.K., F.K., T.K. and B.K.; writing—review and editing, M.K., F.K., T.K. and B.K.; visualization, M.K. and F.K.; supervision, M.K. and F.K.; project administration, M.K. and F.K.; funding acquisition, M.K. All authors have read and agreed to the published version of the manuscript.

Funding: This work was supported in part by the University of Defence within the Organization Development Project VAROPS.

Institutional Review Board Statement: Not applicable.

Informed Consent Statement: Not applicable.

Data Availability Statement: Data are contained within the article.

Conflicts of Interest: The authors declare no conflicts of interest.

Abbreviations

MI-OTA	multiple-input operational transconductance amplifier
CCII	second-generation current conveyor
CFOA	current feedback operational amplifier
VDIBA	voltage differencing inverting buffered amplifier
SIMO	single-input multiple-output
MISO	multiple-input single-output
MIMO	multiple-input multiple-output
MOS	metal oxide semiconductor
MOST	metal oxide semiconductor transistor
CMOS	complementary metal oxide semiconductor
GD	gate-driven
MIBD	multiple-input bulk-driven
TSMC	Taiwan Semiconductor Manufacturing Company
VM	voltage-mode
CM	current-mode
MM	mixed-mode
LPF	low-pass filter
HPF	high-pass filter
BPF	band-pass filter
BSF	band-stop filter
APF	all-pass filter

References

1. Geiger, R.L.; Sánchez-Sinencio, E. Active Filter Design Using Operational Transconductance Amplifiers: A Tutorial. *IEEE Circuits Devices Mag.* **1985**, *1*, 20–32. [CrossRef]
2. Mohan, P.V.A. Generation of OTA-C Filter Structures from Active RC Filter Structures. *IEEE Trans. Circuits Syst.* **1990**, *37*, 656–660. [CrossRef]
3. Laoudias, C.; Psychalinos, C. *Integrated Filters for Short Range Wireless and Biomedical Applications*; Springer: Berlin/Heidelberg, Germany, 2012; pp. 8–9.
4. Lee, C.-N. Fully Cascadable Mixed-Mode Universal Filter Biquad Using DDCCs and Grounded Passive Components. *J. Circuits Syst. Comput.* **2011**, *20*, 607–620. [CrossRef]
5. Minaei, S.; Ibrahim, M.A. A Mixed-Mode KHN-Biquad Using DVCC and Grounded Passive Elements Suitable for Direct Cascading. *Int. J. Circuit Theory Appl.* **2008**, *37*, 793–810. [CrossRef]
6. Alpaslan, H.; Yuce, E. DVCC+ Based Multifunction and Universal Filters with the High Input Impedance Features. *Analog Integr. Circuits Signal Process.* **2020**, *103*, 325–3351. [CrossRef]
7. Yuce, E. Fully Integrable Mixed-Mode Universal Biquad with Specific Application of the CFOA. *AEU-Int. J. Electron. Commun.* **2010**, *64*, 304–309. [CrossRef]
8. Bhaskar, D.R.; Raj, A.; Senani, R. Three New CFOA-Based SIMO-Type Universal Active Filter Configurations with Unrivalled Features. *AEU-Int. J. Electron. Commun.* **2022**, *153*, 154285. [CrossRef]
9. Chen, H.-P.; Wey, I.-C.; Chen, L.-Y.; Wu, C.-Y.; Wang, S.-F. Design and Verification of a New Universal Active Filter Based on the Current Feedback Operational Amplifier and Commercial AD844 Integrated Circuit. *Sensors* **2023**, *23*, 8258. [CrossRef] [PubMed]
10. Pushkar, K.L.; Bhaskar, D.R.; Prasad, D. Voltage-Mode New Universal Biquad Filter Configuration Using a Single VDIBA. *Circuits Syst. Signal Process.* **2014**, *33*, 275–285. [CrossRef]
11. Herencsar, N.; Cicekoglu, O.; Sotner, R.; Koton, J.; Vrba, K. New Resistorless Tunable Voltage-Mode Universal Filter Using Single VDIBA. *Analog Integr. Circuits Signal Process.* **2013**, *76*, 251–260. [CrossRef]
12. Masud, M.I.; A'ain, A.K.B.; Khan, I.A.; Shaikh-Husin, N. CNTFET based Voltage Mode MISO Active Only Biquadratic Filter for Multi-GHz Frequency Applications. *Circuits Syst. Signal Process.* **2021**, *40*, 4721–4740. [CrossRef]
13. Sun, Y.; Fidler, J.K. Design of Current-Mode Multiple Output OTA and Capacitor Filters. *Int. J. Electron.* **1996**, *81*, 95–99. [CrossRef]
14. Abuelma'atti, M.T.; Bentrcia, A. New Universal Current-Mode Multiple-Input Multiple-Output OTA-C Filter. In Proceedings of the 2004 IEEE Asia-Pacific Conference on Circuits and Systems, Tainan, Taiwan, 6–9 December 2004; pp. 1037–1040. [CrossRef]
15. Bhanja, M.; Maity, I.; Roy, M.S.; Ray, B. A Novel Current-Mode Biquadratic OTA-C Filter. In Proceedings of the 2015 IEEE International WIE Conference on Electrical and Computer Engineering (WIECON-ECE), Dhaka, Bangladesh, 19–20 December 2015; pp. 378–381. [CrossRef]
16. Prommee, P.; Pattanatadapong, T. Realization of Tunable Pole-Q Current-Mode OTA-C Universal Filter. *Circuits Syst. Signal Process.* **2010**, *29*, 913–924. [CrossRef]

17. Horng, J.-W. Voltage-Mode Universal Biquadratic Filter with One Input and Five Outputs Using OTAs. *Int. J. Electron.* **2002**, *89*, 729–737. [CrossRef]
18. Lee, W.-T.; Liao, Y.-Z. New Voltage-Mode High-Pass, Band-Pass, and Low-Pass Filter Using DDCC and OTAs. *Int. J. Electron. Commun.* **2008**, *62*, 701–704. [CrossRef]
19. Singh, A.K.; Senani, R.; Bhaskar, D.R.; Sharma, R.K. A New Electronically-Tunable Active-Only Universal Biquad. *J. Circuits Syst. Comput.* **2011**, *20*, 549–555. [CrossRef]
20. Pwint Wai, M.P.; Jaikla, W.; Suwanjan, P.; Sunthonkanokpong, W. Single Input Multiple Output Voltage Mode Universal Filters with Electronic Controllability Using Commercially Available ICs. In Proceedings of the 2020 17th International Conference on Electrical Engineering/Electronics, Computer, Telecommunications and Information Technology (ECTI-CON), Phuket, Thailand, 24–27 June 2020; pp. 607–610. [CrossRef]
21. Lee, C.-N. High-Order Multiple-Mode and Transadmittance-Mode OTA-C Universal Filters. *J. Circuits Syst. Comput.* **2012**, *21*, 1250048. [CrossRef]
22. Rani, N.; Kumar Ranjan, R.; Pal, R.; Paul, S.K. Programmable and Electronically Tunable Voltage-Mode Universal Biquadratic Filter Based on Simple CMOS OTA. In Proceedings of the 2016 3rd International Conference on Devices, Circuits and Systems (ICDCS), Coimbatore, India, 3–5 March 2016; pp. 58–62. [CrossRef]
23. Horng, J.-W. High Input Impedance Voltage-Mode Universal Biquadratic Filter Using Two OTAs and One CCII. *Int. J. Electron.* **2003**, *90*, 183–191. [CrossRef]
24. Raj, A.; Bhaskar, D.R.; Kumar, P. Multiple-Input Single-Output Universal Biquad Filter Using Single Output OTAs. In Proceedings of the 2018 2nd IEEE International Conference on Power Electronics, Intelligent Control and Energy Systems (ICPEICES), Delhi, India, 22–24 October 2018; pp. 1237–1240. [CrossRef]
25. Klungtong, S.; Thanapatay, D. Voltage-Mode Universal Biquadratic Filter Using OTA and Uniform Distributed RC. In Proceedings of the 2013 13th International Symposium on Communications and Information Technologies (ISCIT), Surat Thani, Thailand; 2013; pp. 253–256. [CrossRef]
26. Kumar, K.; Pal, K. Voltage Mode Multifunction OTA-C Biquad Filter. *Microelectron. Int.* **2006**, *23*, 24–27. [CrossRef]
27. Psychalinos, C.; Kasimis, C.; Khateb, F. Multiple-Input Single-Output Universal Biquad Filter Using Single Output Operational Transconductance Amplifiers. *AEU-Int. J. Electron. Commun.* **2018**, *93*, 360–367. [CrossRef]
28. Garradhi, K.; Hassen, N.; Ettaghzouti, T.; Besbes, K. Highly Linear Low Voltage Low Power OTA Using Source-Degeneration Technique and Universal Filter Application. In Proceedings of the 2015 27th International Conference on Microelectronics (ICM), Casablanca, Morocco, 20–23 December 2015; pp. 295–298. [CrossRef]
29. Wang, S.-F.; Chen, H.-P.; Ku, Y.; Yang, C.-M. A Voltage-Mode Universal Filter Using Five Single-Ended OTAs with Two Grounded Capacitors and a Quadrature Oscillator Using the Voltage-Mode Universal Filter. *Opt.-Int. J. Light Electron* **2019**, *192*, 162950. [CrossRef]
30. Tsukutani, T.; Sumi, Y.; Kinugasa, Y.; Higashimura, M.; Fukui, Y. Versatile Voltage-Mode Active-Only Biquad Circuits with Loss-Less and Lossy Integrators. *Int. J. Electron.* **2004**, *91*, 525–536. [CrossRef]
31. Li, S.; Jiang, J.; Wang, J.; Gong, X.; Li, Q. Multiply Universal Filter Based CCCII and OTA Using Minimum Elements. In Proceedings of the 2010 International Conference on Electronic Devices, Systems and Applications, Kuala Lumpur, Malaysia, 1–14 April 2010; pp. 309–312. [CrossRef]
32. Horng, J.-W. Voltage-Mode Universal Biquadratic Filter Using Two OTAs. *Act. Passiv. Electron. Compon.* **2004**, *27*, 835679. [CrossRef]
33. Wang, S.-F.; Chen, H.-P.; Ku, Y.; Yang, C.-M. Independently Tunable Voltage-Mode OTA-C Biquadratic Filter with Five Inputs and Three Outputs and Its Fully-Uncoupled Quadrature Sinusoidal Oscillator Application. *AEU-Int. J. Electron. Commun.* **2019**, *110*, 152822. [CrossRef]
34. Wang, S.-F.; Chen, H.-P.; Ku, Y.; Lin, Y.-C. Versatile Tunable Voltage–Mode Biquadratic Filter and Its Application in Quadrature Oscillator. *Sensors* **2019**, *19*, 2349. [CrossRef]
35. Wang, S.-F.; Chen, H.-P.; Ku, Y.; Lee, C.-L. Versatile Voltage-Mode Biquadratic Filter and Quadrature Oscillator Using Four OTAs and two grounded capacitors. *Electronics* **2020**, *9*, 1493. [CrossRef]
36. Abuelma'atti, M.T.; Bentrcia, A. A Novel Mixed-Mode OTA-C Universal Filter. *Int. J. Electron.* **2005**, *92*, 375–383. [CrossRef]
37. Chen, H.P.; Liao, Y.Z.; Lee, W.T. Tunable Mixed-Mode OTA-C Universal Filter. *Analog Integr. Circuits Signal Process.* **2009**, *58*, 135–141. [CrossRef]
38. Lee, C.N. Multiple-Mode OTA-C Universal Biquad Filters. *Circuits Syst. Signal Process.* **2010**, *29*, 263–274. [CrossRef]
39. Parvizi, M.; Taghizadeh, A.; Mahmoodian, H.; Kozehkanani, Z.D. A Low-Power Mixed-Mode SIMO Universal Gm-C Filter. *J. Circuits Syst. Comput.* **2017**, *26*, 1750164. [CrossRef]
40. Parvizi, M. Design of a New Low Power MISO Multi-Mode Universal Biquad OTA-C Filter. *Int. J. Electron.* **2019**, *106*, 440–454. [CrossRef]
41. Bhaskar, D.R.; Raj, A.; Kumar, P. Mixed-Mode Universal Biquad Filter Using OTAs. *J. Circuits Syst. Comput.* **2020**, *29*, 2050162. [CrossRef]
42. Namdari, A.; Dolatshahi, M. A New Ultra Low-Power, Universal OTA-C Filter in Subthreshold Region Using Bulk-Drive Technique. *AEU-Int. J. Electron. Commun.* **2017**, *82*, 458–466. [CrossRef]

43. Kumngern, M.; Khateb, F.; Kulej, T.; Psychalinos, C. Multiple-Input Universal Filter and Quadrature Oscillator Using Multiple-Input Operational Transconductance Amplifiers. *IEEE Access* **2021**, *9*, 56253–56263. [CrossRef]
44. Jaikla, W.; Khateb, F.; Kumngern, M.; Kulej, T.; Ranjan, R.K.; Suwanjan, P. 0.5 V Fully Differential Universal Filter Based on Multiple Input OTAs. *IEEE Access* **2020**, *8*, 187832–187839. [CrossRef]
45. Namdari, A.; Dolatshahi, M. Design of a Low-Voltage and Low-Power, Reconfigurable Universal OTA-C Filter. *Analog Integr. Circuits Signal Process.* **2022**, *111*, 169–188. [CrossRef]
46. Khateb, F.; Kumngern, M.; Kulej, T.; Akbari, M.; Stopjakova, V. 0.5 V, nW-Range Universal Filter Based on Multiple-Input Transconductor for Biosignals Processing. *Sensors* **2022**, *22*, 8619. [CrossRef]
47. Namdari, A.; Dolatshahi, M.; Aghababaei Horestani, M. A New Ultra-Low-Power High-Order Universal OTA-C Filter Based on CMOS Double Inverters in the Subthreshold Region. *Circuits Syst. Signal Process. Vol.* **2023**, *42*, 6379–6398. [CrossRef]
48. Tlelo-Coyotecatl, E.; Díaz-Sánchez, A.; Rocha-Pérez, J.M.; Vázquez-González, J.L.; Sánchez-Gaspariano, L.A.; Tlelo-Cuautle, E. Enhancing Q-Factor in a Biquadratic Bandpass Filter Implemented with Opamps. *Technologies* **2019**, *7*, 64. [CrossRef]
49. Jendernalik, W.; Jakusz, J.; Blakiewicz, G. Low-Voltage Low-Power Filters with Independent ω_o and Q Tuning for Electronic Cochlea Applications. *Electronics* **2022**, *11*, 534. [CrossRef]
50. Krummenacher, F.; Joehl, N. A 4-MHz CMOS Continuous-Time Filter with On-Chip Automatic Tuning. *IEEE J. Solid-State Circuits.* **1988**, *23*, 750–758. [CrossRef]
51. Khateb, F.; Kulej, T.; Akbari, M.; Tang, K.-T. A 0.5-V Multiple-Input Bulk-Driven OTA in 0.18-μm CMOS. *IEEE Trans. Very Large Scale Integr. (VLSI) Syst.* **2022**, *30*, 1739–1747. [CrossRef]
52. Khateb, F.; Kulej, T.; Kumngern, M.; Psychalinos, C. Multiple-Input Bulk-Driven MOS Transistor for Low-Voltage Low-Frequency Applications. *Circuits Syst. Signal Process.* **2019**, *38*, 2829–2845. [CrossRef]
53. Sun, Y.; Fidler, J.K. Synthesis and Performance Analysis of Universal Minimum Component Integrator-Based IFLF OTA-Grounded Capacitor Filter. *IEE Proc.-Circuits Devices Syst.* **1996**, *143*, 107–114. [CrossRef]
54. Nevárez-Lozano, H.; Sánchez-Sinencio, E. Minimum Parasitic Effects Biquadratic OTA-C Filter Architectures. *Analog Integr. Circuits Signal Process.* **1991**, *1*, 297–319. [CrossRef]